

1
2 **Long-term hydrological changes in northern Iberia (4.9 – 0.9 ky BP)**
3 **from speleothem Mg/Ca ratios and cave monitoring (Ojo Guareña**
4 **Karst Complex, Spain)**

5
6 J.A. Cruz^{1,2}, M.J. Turrero³, J.O. Cáceres⁴, A. Marín-Roldán⁴, A.I. Ortega⁵, A. Garralón³, L.
7 Sánchez³, P. Gómez³, M.B. Muñoz-García¹, R.L. Edwards⁶, J. Martín-Chivelet^{1,2*}

8
9 ¹Departamento de Estratigrafía, Facultad de Ciencias Geológicas, Universidad Complutense de
10 Madrid, 28040 Madrid, Spain

11 ²Instituto de Geociencias (CSIC, UCM), C/José Antonio Nováis 12, 28040 Madrid, Spain

12 ³Departamento de Medioambiente, Ciemat, Avda. Complutense 22, 28040 Madrid, Spain

13 ⁴Departamento de Química Analítica, Facultad de Ciencias Químicas, Universidad Complutense
14 de Madrid, 28040 Madrid, Spain

15 ⁵Department of Geology and Geophysics, University of Minnesota, 310 Pillsbury Drive SE,
16 Minneapolis, MN 55455, USA

17 ⁶Centro Nacional de Investigación sobre la Evolución Humana CENIEH, Paseo Sierra de
18 Atapuerca S/N, 09002 Burgos, Spain

19
20 *e-mail: martinch@ucm.es; phone: +034 913944818; fax: +034 913944798

21
22 **Abstract**

23 An absolute-dated stalagmite from Kaite Cave (Ojo Guareña Karst Complex, N Spain),
24 provides a nearly continuous, high-resolution record of a proxy of regional precipitation patterns
25 through the 4.9 to 0.9 ka BP interval. This record is based in the Mg/Ca ratio of the calcite and
26 its variation through the stalagmite stratigraphy, which is interpreted to be primarily driven by
27 changes in precipitation amount. The calibration of the proxy is supported by the present-day
28 monitoring carried out in the cave for the last 10 years, which reveals a robust inverse
29 relationship between the inter-annual/inter-decadal variability of rainfall and the Mg
30 concentration of dripwaters and precipitating speleothems.

31 The record of paleoprecipitation, based on 2400 Mg/Ca measurements, shows strong variability
32 at inter-annual to inter-decadal scales, and more subtle but significant changes at secular to
33 millennial scales. This long-term paleohydrological evolution outlines five successive intervals
34 with consistent trends, which are bounded by abrupt shifts in the regional precipitation. These
35 shifts took place at 4.65, 4.2, 2.6, and 1.3 ka BP. Significantly, the intervals of maximum
36 precipitation of the whole record (around 4.9-4.65, 2.6-2.45, and 1.3-1.1 ka BP) can be related
37 with episodes of minimum solar activity, and correlated with cold climatic events elsewhere.

38
39 **Keywords:** Speleothem, Karst, Paleohydrology, Mg/Ca, Late Holocene, Iberia.

40
41 **Introduction**

42 The characterization of regional precipitation patterns and changes at decadal to millennial time
43 scales in Europe is of major importance to better understand the evolution of human settlements
44 and societies and to improve the knowledge of the climate system on a synoptic scale. However,

1 information on this climatic parameter beyond the instrumental and historical records is quite
2 scarce because two main reasons: first, the difficulty of getting high resolution, robust
3 paleohydrological records anywhere but particularly in those zones where lakes and wetlands
4 are rare; and second, because the strong spatial variability of rainfall patterns in an area like SW
5 Europe, strongly dependent of the interaction of African subtropical, North Atlantic, and
6 Mediterranean climate systems, which in many cases which in many cases frustrate inter-
7 regional correlations.

8 This study attempts to contribute in this task by yielding a high resolution series for relative
9 paleoprecipitation changes for the northern part of the Iberian Peninsula (4900 to 900 years BP)
10 based on the changes in the magnesium content through a calcite speleothem which grew in
11 Kaite Cave (900 m a.s.l., Ojo Guareña Karst Complex, N Spain). The analysis of variations in
12 the concentration of trace elements such as magnesium during the growth of calcite speleothems
13 has a high potential as a tool for reconstructing past changes in hydrology, rainfall, and
14 temperature (Treble et al. 2003; Johnson et al. 2006; Cruz et al. 2007; Fairchild and Treble
15 2009; Sinclair et al. 2012). These papers also show how that potential is in many cases
16 hampered by the multiple (and in many cases independent) factors that determine the trace
17 element composition of calcite speleothems and the changes in that composition through time. It
18 is for that reason that no general assessments on the hydrological or geochemical functioning of
19 karst systems from a particular emplacement can be made. One part of this hindrance is being
20 solved by progress in experimental laboratory work, which allows for example a better
21 understanding of the factors that modulate the distribution coefficient of each element (e.g.,
22 Gascoyne, 1983; Huang and Fairchild 2001, Day and Henderson 2013, Nielsen 2013). Progress
23 can also be made by a rigorous calibration of the signal recorded by the speleothem by means of
24 contemporary Mg/Ca time-series data in the specific conditions of each cave and the routing
25 system of percolating waters until the place of calcite precipitation (e.g., Tremaine and Froelich
26 2013). In this sense, our paleoclimate interpretation of the magnesium concentration variation
27 through the studied speleothem is supported by a long-term monitoring program (10 years)
28 performed in the cave from where the stalagmite was retrieved.

29 The studied stalagmite provides a nearly continuous record of the paleohydrological conditions
30 of N Spain over the covered time interval. The series was constructed on a robust time model
31 supported by precise ^{230}Th absolute dating, and the magnesium content is expressed by Mg/Ca
32 ratios of nearly 2400 analyses performed through the stalagmite by means of Laser Induced
33 Breakdown Spectroscopy (LIBS). The potential of this analytical technique, only tentatively
34 used in speleothem research (e.g., Vadillo et al. 1998; Fortes et al. 2012; Marín-Roldán et al.
35 2014), is also explored and discussed in the paper.

37 **Sampling site and studied material**

39 The speleothem studied in this paper, named Buda-100, is a cylindrical and very elongated (112
40 cm long \times 4–6 cm thick) stalagmite, which was retrieved from the Buda Hall in the Kaite Cave
41 (Ojo Guareña Karst Complex, Burgos Province, N Spain, Fig. 1). The sample, fallen and broken
42 in several pieces when collected, was reconstructed and then cut in two longitudinal halves.
43 These pieces (and 19 petrographical thin sections made from them) are preserved in the
44 collection of the Department of Stratigraphy of the Complutense University of Madrid. Buda-
45 100 exclusively consists of calcite and shows two main microfabrics: columnar fibrous calcite
46 (mainly in their axial part), and dendritic in some peripheral areas. Its internal stratigraphy is
47 quite complex in the central part, but much simpler in the periphery, where a pervasive pattern
48 defined by a sub-millimetric lamination is shown. This lamination, according to the age model
49 and the microstratigraphic analysis, is interpreted as annual in origin.

50 Kaite Cave is quite small (~350 m of maximum length) and relatively shallow (12-20 m below
51 the surface), and is topographically isolated from the main levels of the Ojo Guareña Karst
52 Complex. The cave is 860 m above sea level and the area has a relatively humid, temperate

1 climate. The region is located in the transition between the two main climatic zones of Western
2 Europe: the Atlantic and the Mediterranean. The climate is warm-temperate, with annual mean
3 temperatures in the range of 10-11 °C, although these vary notably according the seasons (with
4 mean temperatures over 18 °C in July-August, and less than 5°C in January-February). The
5 annual precipitation averages ~720mm (1990–2014 interval, Villarcayo Meteorological Station,
6 Agencia Estatal de Meteorología (AEMET) and Confederación Hidrográfica del Ebro (CHE),
7 W3°34'20" N42°56'26", 595 m a.s.l.), with maximum precipitation in November to January but
8 also notable precipitation in April-May, and quite dry summers. During winter, part of the
9 precipitation is snow, which never lasts on the ground more than several days or few weeks.
10 The soil above the cave is shallow (essentially a lithosol) with scarce argillaceous material and
11 organic matter. However, it allows the development of a quite dense cover of small *Quercus* and
12 *Juniperus*. The cave is developed on lightly dipping carbonate unit of Upper Cretaceous
13 (Coniacian) age, which consists of shallow marine, partially dolomitized limestone.

14 The monitoring program commenced in 2002 at Las Velas Hall, a small gallery adjacent to
15 Buda Hall, both separated ~340 m from the main entrance. The monitoring site is characterized
16 by a stable cave climate: the temperature is 10.40 ± 0.04 °C and reflects the mean annual
17 temperature outside the cave, the relative humidity exceeds always 99 % and there are no
18 significant air currents (Turrero et al. 2004; 2007).

19 The seepage water is frequent, with permanent but variable dripping during the year with a
20 definite seasonal effect, and the speleothems are abundant, some of which are growing at the
21 present time. The total volume of dripping water collected seasonally is consistent with an
22 advective flow through the surrounding rock. The data presented in this work correspond to 10
23 years of monitoring of two points with a “low” and “rapid” flow, with an average annual drip
24 rate of ~ 0.02 mL/min and ~ 0.58 mL/min, respectively.

25

26 **Methods**

27

28 ²³⁰Th age-dating

29

30 Radiometric ages of speleothem calcite can be obtained efficiently with the application of U-
31 series dating techniques on inductively coupled plasma mass spectrometers (ICP-MS) (Shen et
32 al. 2002). With this aim, 14 samples of approximately 150-200 mg of calcite powder were
33 extracted along selected stratigraphic intervals from stalagmite Buda-100 and prepared for ²³⁰Th
34 dating according to the procedures described by Edwards et al. (1987) and Dorale et al. (2004).
35 ICP-MS analyses of stalagmite Buda-100 samples were performed at the Minnesota Isotope
36 Laboratory on a multi-collector inductively coupled plasma mass spectrometer (MC-ICP-MS,
37 Thermo Finnigan Neptune) using a MasCom multiplier behind the retarding potential
38 quadrupole (RPQ).

39 The analytical work of Buda-100 was accompanied by the petrographic study of the speleothem,
40 in order to recognize its internal stratigraphy (e.g., identification of hiatuses and growth
41 patterns), and to detect possible diagenetic features (e.g., micro-dissolution, internal carbonate
42 precipitation, incipient recrystallization). This study was useful in the selection of the extraction
43 points of subsamples for absolute age-datings as well as transects for trace element analyses.

44

45 Mg/Ca measurements

46

47 Determination of Mg geochemical data in Buda-100 was conducted by laser induced breakdown
48 spectroscopy (LIBS) (Fig. 2a), at the Complutense University of Madrid in the Department of
49 Analytical Chemistry, using a Q-switched Nd:YAG laser (Quantel, Brio model) operating at

1 1,064 nm, with a pulse duration of 4 ns. The analyses were performed on the polished surface of
2 the 19 thin sections (mounted on 5x8 cm slabs, 500 μm thick) prepared for petrographical and
3 geochemical analyses (Fig. 2b). Each thin section was placed over an X–Y–Z manual micro-
4 metric positionator with a 0.5 mm stage of travel at every coordinate to ensure that each laser
5 pulse impinged on the speleothem. The laser beam was focused on the surface of the speleothem
6 with a 100 mm focal-distance lens. This large working distance allowed easy sample
7 manipulation and plasma light collection while the focusing provided by the lens enabled
8 extremely precise placement of the beam on the speleothem. Emission from the plasma was
9 collected, and then focused into an optical fiber, coupled to a spectrometer. The spectrometer
10 system was a user-configured miniature single-fiber system EPP2000 StellarNet (Tampa, FL,
11 U.S.A.) with a charged coupled device detector (CCD) with a spectral resolution of ± 0.5 nm.
12 The wavelength range used was from 200 to 1,000 nm. The detector integration time was set to
13 100 ms. Each point analyzed was exposed to 3 laser shots before performing the measurements
14 to eliminate any impurity on the surface. The recorded spectra are the average of 20 laser pulses
15 at each single position (Fig. 2c and d). The lateral resolution between spectra was established at
16 500 μm . The spectral data was processed using an interface created in Matlab software. LIBS
17 data are shown as the ratio of the intensity of Mg versus Ca, Ca being the internal standard. This
18 option is a preventive measure to minimize alteration that can affect the LIBS signal, because of
19 laser-matter interaction during laser ablation. These alterations can be originated by
20 heterogeneity, roughness, variations in the microporosity, etc. of the speleothem surface.

21 Marín-Roldán et al. (2014) propose a series of experimental proofs to check the quality and
22 reliability of trace element data obtained by LIBS in speleothems. These include tests for (a)
23 uniform plasma temperature (no significant variation in the temperature of the plasma during
24 the experimental measurements allows accurate comparison between the emission intensity of
25 the spectral lines and the corresponding analytical response); (b) homogeneity of data along
26 single growth layers (the absence of significant lateral changes in the trace element composition
27 would allow to recognize the data as representative of each growth layer); and (c) repeatability
28 of the measurements (and the resulting series). These three tests were performed during the
29 measurements with positive results, which are illustrated in Figures 3a, b, and c.

30 Additionally, the reliability of the LIBS Mg/Ca data was checked by independent analyses, for
31 selected intervals of the stalagmite, by inductively coupled plasma-optical emission
32 spectroscopy (ICP-OES), a more traditional technique which requires of larger amounts of
33 sample (consequently losing the LIBS micrometric resolution). We used a spectrometer Perkin
34 Elmer ICP-OES 5200 DV in the National Research Center of Human Evolution (CENIEH) in
35 Burgos (Spain), which yielded values of Mg in the speleothem of 150 to 400 ppm. The samples
36 analyzed by ICP-OES were drilled using 0.5mm carbide dental burns, sampling areas of
37 4x4mm, to get approximately 3-8mg of sample. That means that the analytical results yielded
38 by this technique represent non-weighted averages of about 10-20 annual growth layers,
39 whereas the results from LIBS come from about 30 micrograms, and correspond to growth time
40 intervals of several months. Because the very different size of the samples, perfect matches
41 between LIBS and ICP-OES curves should not be expected. However, comparable trends
42 between the two records have been obtained in our study (Fig. 3d).

43 The positive results in the LIBS evaluation tests (*sensu* Marín-Roldán et al. 2014) and the
44 reasonably good correlation (with the explained limitations) of LIBS and ICP-OES data support
45 our argument that the Mg/Ca measurements for obtaining the time series are representative of
46 the changes in the Mg content in the speleothem through time and can be used for paleoclimate
47 interpretation.

48 Related to water samples from contemporary monitoring, aliquots representative of the total
49 amount of the seasonal sampling for each drip point were filtered through Millipore filters with
50 pore size 0.45 μm for complete chemical characterization. Magnesium and calcium were
51 analyzed by ion chromatography with METROHM equipment with high-performance Metrosep
52 C3-250 column. Data quality was assessed by replicate samples and sample blanks.

1
2
3
4
5
6
7
8
9
10
11
12
13
14
15
16
17
18
19
20
21
22
23
24
25
26
27
28
29
30
31
32
33
34
35
36
37
38
39
40
41
42
43
44
45
46
47
48
49

Cave monitoring: Mg/Ca – climate relationship

Mg content in the calcite of stalagmites is given by the distribution coefficient $K_{Mg} = (Mg/Ca)_{calcite}/(Mg/Ca)_{solution}$. Because K_{Mg} is modulated by temperature, the Mg/Ca ratio in speleothems was considered as a possible paleothermometer in pioneer works (e.g., Gascoyne, 1983). However, according to the experimental work by Huang and Fairchild (2001) about the temperature-dependence of K_{Mg} under laboratory conditions, the temperature variations in the Kaite Cave estimated for the late Holocene (Martin-Chivelet et al. 2011), would be too small to generate significant changes in the Mg/Ca ratios through time in stalagmite such as Buda-100. For this reason, K_{Mg} can be assumed to be roughly constant through time, and thus, the changes in the Mg/Ca in speleothem series should be regarded through the time variability in the hydrochemistry of the cave drip-waters.

These changes in the composition of the drip-water could be related to various processes acting in Kaite Cave:

(a) Differential rates of dissolution of calcite and dolomite in the bedrock, which is favored in the case of Kaite Cave by the mixed dolomitic–calcitic nature of the Cretaceous carbonates. Because of the Mg content of dolomite, this process will affect near exclusively to this element: the aqueous leachates should have lower Mg/Ca relative to the bedrock because of preferential calcite dissolution, but that ratio can rise by increasing water residence times, an aspect that took place during the drier time intervals when the seepage flow decreases. Similar cases were described by Fairchild et al. (2000).

(b) Prior calcite precipitation (PCP), which is favored by the climatic conditions of the Kaite area (Turrero et al. 2015). When percolating, the waters can pass from a dissolution regime to a precipitation regime as they get into areas with lower pCO_2 than that which they have previously equilibrated. The resultant degassing leads to calcite precipitation and, consequently also to water enrichment in Mg relative to Ca. PCP is enhanced during dry climatic periods (e.g., Fairchild and Treble 2009), and thus, the higher values in Mg of the dripwaters and of the speleothems should reflect climatic conditions of low rainfall.

The hydrochemical monitoring in Las Velas Hall (Kaite) for the 2002 -2012 interval shows distinctive patterns for both the drip-rate and the Mg/Ca molar ratio in the drip-water (Fig. 4). These patterns are defined by a net progressive increase for the Mg/Ca molar ratio and a negative trend for the drip-rate.

It should be noted that calcium in dripwaters of Kaite does not correlate with magnesium ($r = 0.12$), reflecting that dripwater should not be affected by dilution processes when rainfall increases (Tooth and Fairchild 2003; Baldini et al. 2006), so attention should be paid to dissolution-precipitation processes in the epikarst and the vadose zone affecting the dripwater chemistry.

For a meaningful understanding of these Mg/Ca variations from a hydrological perspective, the inter-decadal rainfall evolution pattern for the area must be considered. A recent study (Confederación Hidrográfica del Ebro, 2012) based in the regional integration and homogenization of meteorological data from 29 observatories, shows a significant decreasing trend in annual rainfall over the Kaite Cave area during the last four decades. Specifically, for the interval 1990-2010 an average annual decrease of -0.7%/year is reported. At a seasonal scale, significant rainfall decrease took place during spring (averaging -2.5%/year), summer (-0.9%/year) and autumn (-0.7%/year) rainfall, while winter rainfall increases (1.3%/year). Our own data, limited to the last ten years, are in accordance with those values.

The decreasing trend in annual rainfall over the Kaite Cave area in recent years coincides with a trend of decreasing drip-rates at the two monitored points in Las Velas Hall (Fig. 4),

1 demonstrating the link between regional scale hydrological conditions, drip-rates and water
2 chemistry.

3 Since lower rainfall means less water available for recharging the system, the coexistence of a
4 sharp increase of the Mg/Ca ratio together to a drip-rate decrease points towards changes in the
5 epikarst through water-rock interaction processes. Prior calcite precipitation in the epikarst
6 and/or unsaturated zone is invoked as the process causing progressive increasing in the Mg/Ca
7 molar ratio. It means that a significant storage may occur in the matrix, and in other parts of the
8 system, like the epikarst driving slow fluxes and giving time to the above described processes.

9 Prior calcite precipitation is considered a long-term (years) water-rock interaction process as a
10 consequence of a continuous decreasing of recharge in the area as reflected during the analyzed
11 period. At seasonal scale lower rainfall during spring, summer and autumn lead to lower
12 recharge and increase of the effect of prior calcite precipitation, being the general inter-annual
13 trend superimposed to that seasonal trend.

14

15 **Stalagmite age model**

16

17 A total of fourteen ²³⁰Th dates were determined for Buda-100 (Table 1). All ages are in correct
18 stratigraphic order and suggest quite constant growth rates for the stalagmite. Petrographic
19 analyses indicate complex internal growth patterns in some parts of the stalagmite but a net
20 continuous growth. Minor hiatal surfaces punctuated the microstratigraphic series. Because their
21 duration is short and difficult to estimate (probably in the range of few years), these hiatuses
22 were not incorporated into the age model. A former chronostratigraphy of the stalagmite based
23 in preliminary data (Cruz et al. 2015), clearly overestimated the duration of two of these
24 surfaces. The age model for this stalagmite was performed by applying the StalAge algorithm
25 (Scholz and Hoffmann 2011). According to this model (Fig. 5) Buda-100 grew between
26 4900±50 and 950±170 years BP, covering four millennia in the middle to late Holocene.
27 Calculated growth rates are essentially constant through the four millennia, averaging 0.3
28 mm/year, with two minor exceptions: the rates can exceed 0.5 mm/year in the centuries around
29 3800 years BP and are as low as to 0.1 mm/year in the last 150 years of the record.

30

31 **The Mg/Ca series**

32

33 2400 Mg/Ca LIBS measurements were performed along Buda-100 and then time-scaled
34 according to the age model to construct the time series of Figure 5. The Mg/Ca intensity ratio
35 averages 0.05 and ranges from 0.02 to 0.13. The series is characterized by a noticeable
36 variability at the shortest timescales, which should be induced mainly by seasonal and
37 interannual changes in the speleothem composition. That variability, of great interest, will not
38 be analyzed in this paper, as further microstratigraphic work is required for its correct
39 understanding. Superimposed on that high frequency variability, longer-term, more subtle
40 changes can be recognized in the speleothem Mg/Ca record. For visually analyzing the longer
41 term changes, the series was smoothed by means of a simple 9-term running average (Fig. 6).
42 Additionally, a spectral analysis was performed on the bulk time series for the identification of
43 cyclic patterns in the Mg/Ca variability. This analysis was performed by means of the Lomb
44 periodogram algorithm, indicated for unevenly spaced time series, and was made with the aid of
45 the PAST software (Hammer et al., 2006). A minor mathematical treatment of the data set was
46 introduced on the original data set prior to the analysis, with the aim of eliminating its long-term
47 positive trend. It was made by subtracting the best-fit linear function from the data. The result,
48 shown in the spectral diagram of Fig. 7, reveals a very significant spectral peak for a period of
49 210 years, as well as secondary but also significant peaks for 725, 578, 445, 255, and 99
50 years. The Mg/Ca record is interpreted in terms of paleohydrological changes that occurred in

1 the region of the cave through time. Variations in the Mg/Ca of the speleothem are mainly
2 determined by the composition of drip-waters, and this composition is strongly dependent of the
3 water-rock interaction occurring in the epikarst. Larger residence times would result in
4 enrichment in Mg/Ca of the water, as a result of several processes which include prior calcite
5 precipitation and/or differential dissolution of calcite and dolomite in the bedrock. Because
6 residence times decrease with higher water recharge, and the recharge depends of the annual
7 amount of precipitation (mainly autumn- winter-spring), the Mg content in the calcite of the
8 speleothem correlates inversely with that meteorological parameter. However, the complex
9 nature of the Mg/Ca record and the inherent limitations of present day monitoring, permit
10 neither the proposal of an absolute quantification nor the calibration of the paleohydrological
11 changes reconstructed from the Mg/Ca record. These are interpreted in terms of “relative”
12 paleoprecipitation variations, e.g., drier or wetter intervals.

13 It should be noted, however, that despite the noticeable variability of the record over those four
14 millennia, the broad climatic conditions remained quite stable, and that such precipitation
15 variability should occur in a relatively narrow range. Buda-100 stratigraphy reflects (beyond the
16 Mg/Ca variability) that the paleohydrological conditions were stable enough to allow a nearly
17 continuous stalagmite growth at remarkably homogeneous growth rates. And this aspect
18 suggests that, even during the driest periods, the climate was humid enough to allow significant
19 water recharge to maintain stable dripping on the stalagmite.

20

21 **Paleohydrological intervals and events**

22

23 The Mg/Ca series defines five long-term paleohydrological intervals of moderate amplitude if
24 compared with the high-frequency variability, but with well-outlined trends (Fig. 6). They are
25 bounded by significant events. From older to younger, these intervals and events are:

26 -1st Interval (4.9-4.65 ka BP): This period is defined by the lowest values in the Mg/Ca ratios,
27 i.e., the climatic conditions are prevailingly wet. No positive or negative trend is clearly
28 appreciated within this interval. Comparing with other areas and proxies, this time is broadly
29 accepted to be a cold episode, and negative temperature anomalies have been reported in
30 Greenland, North America, Africa, and Antarctica (e.g., Wanner et al. 2011, and references
31 therein). In Europe less clear anomalies in the temperatures have been stated, but a notable
32 glacier advance in the Alps has been recently reported between 4.8 and 4.6 ka BP (Luetscher et
33 al. 2011) and an important humid period has been recognized in the eastern Mediterranean
34 (Triantaphyllou et al. 2014).

35 -Event at 4.65 ka BP. In the stalagmite record, it is marked by an abrupt and intense increase in
36 the Mg/Ca, i.e., a very rapid shift toward drier conditions.

37 -2nd Interval (4.65-4.2 ka BP): After the 4.65 ka BP event, the Mg/Ca values stay high for
38 approximately two centuries and then started to gradually decrease until the end of the interval.
39 This indicates that, after an initial dry period, the regional climate evolves gradually to more
40 humid conditions. Maximum precipitation was reached at the end of the interval (4.2 ka BP).
41 This whole interval has been considered as cold in northern Europe, with rapid advance of
42 glaciers and the onset of the so-called Neoglacial period. Contrarily to our stalagmite record, in
43 other areas the 4.2 ka BP wet episode is defined by strong dryness, such as in North America
44 (Booth et al. 2005), Mexico (Bernal et al. 2011), the Middle-Est (Weiss et al. 1993; deMenocal
45 2001; Ayalon and Bar-Matthews 2011), and China (Wang et al. 2005).

46 -3rd Interval (4.2-2.65 ka BP): The boundary with the previous interval is not marked by an
47 abrupt shift (or event), but by a net change in the trend. After several decades of humid
48 conditions around 2.4 ka BP, the conditions change towards a greater dryness. In fact, this 3rd
49 interval is very long and defined by a net positive trend in the Mg/Ca values (i.e. drier
50 conditions). It shows an internal complex variability, punctuated by several secular episodes of
51 greater dryness (around 3.7 and 3.3 ka BP).

1 -Event at 2.65 ka BP: Short interval (few decades) defined by an abrupt decrease in the Mg/Ca,
2 which returns to the low values of the onset of the series and the start of the previous interval.
3 This event records a major regional paleohydrological change, with an abrupt increase in
4 precipitation. It can be correlated with episodes of rapid climate change (cooling) in central
5 Europe (e.g., Swindles et al. 2007; Martin-Puertas et al. 2012, Wanner et al. 2011; 2014; and
6 references therein).

7 -4th Interval (2.6-1.35 ka BP): After the abrupt decrease in the Mg/Ca of the 2.6 ka event,
8 another prolonged interval began, being again defined by a net positive trend in the Mg/Ca
9 series (dryness increase). The fourth interval (2.6 ka – 1.35 ka BP) starts with a 150 yr period of
10 wet conditions followed by a long interval during which the conditions progressively became
11 drier. This interval coincides with the progressive aridification recognized in the western
12 Mediterranean area, conditions which seem to have preceded and accompanied the
13 Romanization of Iberia (Jalut et al. 2000; 2009). The late part of this interval is commonly
14 identified in Europe with the Dark Ages or the Migration Period Cooling (Ljungqvist 2010),
15 with strong human migratory movements.

16 -Event at 1.35 ka BP: Shift defined by a rapid decrease in the Mg/Ca (which however does not
17 reach values as lower as in the previous events) which abruptly ended the previous dry period.

18 -5th Interval (1.3-1.0 ka BP): This final period is defined by remarkably low values in the Mg/Ca
19 ratios during the first ~200 years (wet conditions), and a later interval for which the Mg content
20 starts to increase (drier conditions). A marked humid event, however, is recognized around 1.15
21 ka BP. The end of this interval, with a clear positive trend, is defined by the top of the
22 stalagmite record. Interestingly, the climatic conditions in this time interval experienced an
23 abrupt change in Europe, which derived in the so-called Medieval Climate Anomaly (MCA).
24 The MCA, which lasted from the 8th to the 14th Century (Martín-Chivelet et al., 2011), was
25 characterized by changes in climate globally, including relative warmth over the North
26 Atlantic/European region and much of the extra-tropical Northern Hemisphere (Esper et al.
27 2002). The reason why the stalagmite stopped growing remains unclear. The high Mg/Ca values
28 and the final positive trend in the Mg/Ca, coupled with slow speleothem growth rates suggest
29 that the end of the stalagmite development could be related to a reduction of water availability
30 in the cave as a result of a dry period. Trouet et al. (2009) demonstrates that the MCA was
31 characterized by a period of persistent positive North Atlantic Oscillation (NAO) probably
32 starting before 1000 yr BP. This positive phase could determine prolonged dry winter
33 conditions in SW Europe and the Mediterranean.

34 These paleohydrological intervals should be framed within the variability of the N Atlantic and
35 European climates during the Late Holocene. For the considered interval, the proposed main
36 forcing of climate change is the solar activity (e.g., Wanner et al. 2014). In this sense, we must
37 emphasize that the three episodes of maximum pluviosity recognized in our stalagmite record
38 can be related with periods of Grand Solar Minima (GSM). This correlation points towards a
39 strong coupling between solar activity and precipitation over northern Iberia. Three main GSM
40 occurred during the considered interval, dated at 4.9, 2.8 and 1.3 ka BP (Steinhilber et al. 2009).
41 Two of these GSM (4.9 and 1.3 ka BP) coincides precisely with the onset of two our maximum
42 pluviosity intervals, indicating a rapid and robust response of the paleohydrological regime to
43 the solar activity decrease. The third GSM (2.8 ka BP, 'Homeric Minimum') can be also related
44 with the maximum pluviosity episode that started several decades later, at ~2.65 ka BP.
45 Interestingly, a similar delay was postulated by Swindles et al. (2007) in a well age-constrained
46 continental record in Ireland, where a major paleohydrological shift (to wetter/cooler
47 conditions) also postdated the 2.8 ka BP solar minimum.

48 Additionally, the spectral analysis of the Mg/Ca time series (Fig. 7) revealed a preponderant
49 cyclicity (maximum spectral power peak) for 210 years (as well as secondary ones for 725, 578,
50 445, 255, and 99 years). Significantly, that dominant cyclicity in BUDA-100 Mg/Ca record has
51 a comparable period to the Suess solar cycle, recognized by different authors in cosmogenic
52 isotopes records in tree rings and ice-cores (e.g., Dergachev et al. 2000; Vasiliev and Dergachev

1 2002; Steinhilber et al. 2009). Although the relationships between the Mg/Ca record and the
2 solar cycles need to be further investigated, the identification of frequencies typical of solar
3 cycles in the speleothem record also argues for a strong influence of solar activity changes in the
4 rainfall patterns of SW Europe.
5

6 7 **Conclusions**

8
9 -The Holocene stalagmite Buda-100, retrieved from the Kaite Cave (Ojo Guareña Karst
10 Complex, N Spain) was radiometrically dated by ^{230}Th and analyzed by laser induced
11 breakdown spectroscopy (LIBS) for obtaining a high-resolution series of Mg/Ca ratios.

12 -The stalagmite, which grew from 4.9 to 0.9 ka BP, show significant variations of Mg/Ca,
13 which are primarily driven by changes in the precipitation amount. The calibration of the proxy
14 is supported by the present-day monitoring carried out in the cave for the last 10 years, which
15 reveals a strong inverse relationship between the inter-annual variability of rainfall (and drip-
16 rate) and the Mg concentration of drip-waters and precipitating speleothems.

17 -The record of paleoprecipitation, based in 2400 Mg/Ca measurements, outlines five successive
18 paleohydrological intervals with consistent trends, and bounded by events that define abrupt
19 shifts in paleoprecipitation. These took place at 4.65, 4.2, 2.6, and 1.3 ka BP.

20 -Significantly, the intervals of maximum precipitation of the whole record (around 4.9-4.65,
21 2.6-2.45, and 1.3-1.1 ka BP) can be related with Grand Solar Minima (GSM), and correlated
22 with cold climatic events elsewhere.
23

24 **Acknowledgments**

25
26 We greatly appreciate the invitation to contribute to this special issue by the invited editors, and
27 the comments and suggestions by two anonymous referees. Contribution to research projects
28 CGL2010-21499-BTE and CGL2013-43257-R of the Spanish R+D National Program
29 (MINECO) and research groups “Paleoclimatology and Global Change” and “Laser Induced
30 Breakdown Spectroscopy (LIBS)” from the UCM (Spain). We thank the facilities and
31 permissions given by the Junta de Castilla y León (Spain) for accessing and working in the Ojo
32 Guareña Natural Monument. The collaboration of the Grupo Espeleológico Edelweiss (Exma.
33 Dip. Prov. Burgos) is also greatly acknowledged. Thanks are extended to S. Moncayo and S.
34 Manzoor for their help and advice in this work.
35

36 **References**

37
38 Ayalon A, Bar-Matthews M (2011) Mid-Holocene climate variations revealed by high-
39 resolution speleothem records from Soreq Cave, Israel and their correlation with cultural
40 changes. *The Holocene* 21:163-171. doi:10.1177/0959683610384165

41 Baldini JUL, McDermott F, Fairchild IJ (2006) Spatial variability in cave drip water
42 hydrochemistry: Implications for stalagmite paleoclimate records. *Chem Geol* 235: 390-404.
43 doi: 10.1016/j.chemgeo.2006.08.005

- 1 Bernal JP, Lachniet M, McCulloch M, Mortimer G, Morales P, Cienfuegos E (2011) A
2 speleothem record of Holocene climate variability from southwestern Mexico. *Quaternary Res*
3 75:104-113. doi:10.1016/j.yqres.2010.09.002
- 4 Booth RK, Jackson ST, Forman SL, Kutzbach JE, Bettis III EA, Kreig J, Wright DK (2005). A
5 severe centennial-scale drought in mid-continental North America 4200 years ago and apparent
6 global linkages. *The Holocene* 15, 321-328. doi: 10.1191/0959683605hl825ft
- 7 Cheng H., Edwards RL, Hoff J, Gallup CD, Richards DA, Asmerom Y (2000) The half-lives of
8 uranium-234 and thorium-230. *Chem Geol* 169: 17–33. doi:10.1016/S0009-2541(99)00157-6
- 9 Confederación Hidrográfica del Ebro (2012) Evolución de la temperatura y la precipitación en
10 la cuenca del Ebro. www.chebro.es
- 11 Cruz JA, Martín-Chivelet J, Marín-Roldán A, Turrero MJ, Edwards RL, Ortega AI, Cáceres JO
12 (2015) Trace Elements in Speleothems as Indicators of Past Climate and Karst Hydrochemistry:
13 A Case Study from Kaite Cave (N Spain). In: Andreo B, Carrasco F, Durán JJ, Jiménez P,
14 LaMoreaux JW (eds) *Hydrogeological and Environmental Investigations in Karst Systems*, vol
15 1. *Environ Earth Sci*. Springer Berlin Heidelberg, pp 569-577. doi:10.1007/978-3-642-17435-
16 3_64
- 17 Cruz Jr FW, Burns SJ, Jercinovic M, Karmann I, Sharp WD, Vuille M (2007) Evidence of
18 rainfall variations in Southern Brazil from trace element ratios (Mg/Ca and Sr/Ca) in a Late
19 Pleistocene stalagmite. *Geochim Cosmochim Acta* 71:2250-2263.
20 doi:10.1016/j.gca.2007.02.005
- 21 Day CC, Henderson GM (2013) Controls on trace-element partitioning in cave-analogue calcite.
22 *Geochimica et Cosmochimica Acta* 120:612-627. doi: 10.1016/j.gca.2013.05.044
- 23 deMenocal PB (2001) Cultural Responses to Climate Change During the Late Holocene.
24 *Science* 292:667-673. doi:10.1126/science.1059287
- 25 Dergachev VA, Raspopov OM, Vasiliev SS (2000) Long-term variability of solar activity
26 during the Holocene. Proc. 1st Solar & Space Weather Euroconference, “The Solar Cycle and
27 Terrestrial Climate”, Santa Cruz de Tenerife, Spain (ESA SP-463, December 2000).
- 28 Dorale J, Edwards RL, Alexander EC, Jr., Shen C-C, Richards D, Cheng H (2004) Uranium-
29 Series Dating of Speleothems: Current Techniques, Limits, & Applications. In: Sasowsky I,
30 Mylroie J (eds) *Stud Cave Sediments*. Springer US, pp 177-197. doi:10.1007/978-1-4419-9118-
31 8_10
- 32 Edwards RL, Chen JH, Wasserburg GJ (1987) ^{238}U ^{234}U ^{230}Th ^{232}Th systematics and the precise
33 measurement of time over the past 500,000 years. *Earth Planet Sc Lett* 81:175-192.
34 doi:10.1016/0012-821X(87)90154-3
- 35
- 36 Esper J, Cook ER, Schweingruber FH (2002) Low-Frequency Signals in Long Tree-Ring
37 Chronologies for Reconstructing Past Temperature Variability. *Science* 295 (5563): 2250-2253.
38 doi: 10.1126/science.1066208
- 39 Fairchild IJ, Borsato A, Tooth AF, Frisia S, Hawkesworth CJ, Huang Y, McDermott F, Spiro B
40 (2000) Controls on trace element (Sr–Mg) compositions of carbonate cave waters: implications
41 for speleothem climatic records. *Chem Geol* 166:255-269. doi:10.1016/S0009-2541(99)00216-8

- 1 Fairchild IJ, Treble PC (2009) Trace elements in speleothems as recorders of environmental
2 change. *Quaternary Sci Rev* 28:449-468. doi:10.1016/j.quascirev.2008.11.007
- 3 Fortes FJ, Vadillo I, Stoll H, Jimenez-Sanchez M, Moreno A, Laserna JJ (2012) Spatial
4 distribution of paleoclimatic proxies in stalagmite slabs using laser-induced breakdown
5 spectroscopy. *J Anal Atom Spectrom* 27:868-873. doi:10.1039/c2ja10299d
- 6 Gascoyne M (1983) Trace-element partition coefficients in the calcite-water system and their
7 paleoclimatic significance in cave studies. *J Hydrol* 61:213-222. doi:10.1016/0022-
8 1694(83)90249-4
- 9 Hammer Ø, Harper DAT, Ryan PD (2006) PAST - PALaeontological STatistics, ver. 1.58.
10 December 7, 2006
- 11 Huang Y, Fairchild IJ (2001) Partitioning of Sr²⁺ and Mg²⁺ into calcite under karst-analogue
12 experimental conditions. *Geochim Cosmochim Acta* 65:47-62. doi:10.1016/S0016-
13 7037(00)00513-5
- 14 Jalut G, Dedoubat JJ, Fontugne M, Otto T (2009) Holocene circum-Mediterranean vegetation
15 changes: Climate forcing and human impact. *Quatern Int* 200:4-18
16 doi:10.1016/j.quaint.2008.03.012
- 17 Jalut G, Esteban Amat A, Bonnet L, Gauquelin T, Fontugne M (2000) Holocene climatic
18 changes in the Western Mediterranean, from south-east France to south-east Spain *Palaeogeogr*
19 *Palaeocl* 160:255-290 doi:10.1016/S0031-0182(00)00075-4
- 20 Johnson KR, Hu C, Belshaw NS, Henderson GM (2006) Seasonal trace-element and stable-
21 isotope variations in a Chinese speleothem: The potential for high-resolution paleomonsoon
22 reconstruction *Earth Planet Sc Lett* 244:394-407 doi:10.1016/j.epsl.2006.01.064
- 23 Ljungqvist FC (2010) A new reconstruction of temperature variability in the extra-tropical
24 northern hemisphere during the last two millennia. *Geografiska Annaler: Series A, Physical*
25 *Geography* 92:339-351. doi:10.1111/j.1468-0459.2010.00399.x
- 26 Luetscher M, Hoffmann DL, Frisia S, Spötl C (2011) Holocene glacier history from alpine
27 speleothems, Milchbach cave, Switzerland. *Earth Planet Sc Lett* 302:95-106.
28 doi:10.1016/j.epsl.2010.11.042
- 29 Marín-Roldán A, Cruz JA, Martín-Chivelet J, Turrero MJ, Ortega AI, Cáceres JO (2014)
30 Evaluation of Laser Induced Breakdown Spectroscopy (LIBS) for detection of trace element
31 variation through stalagmites: potential for paleoclimate series reconstruction. *J Appl Las*
32 *Spectrosc* 1:7-12
- 33 Martín-Chivelet J, Muñoz-García MB, Edwards RL, Turrero MJ, Ortega AI (2011) Land
34 surface temperature changes in Northern Iberia since 4000 yr BP, based on δ¹³C of
35 speleothems. *Global Planet Change* 77:1-12. doi:10.1016/j.gloplacha.2011.02.002
- 36 Martín-Puertas C, Matthes K, Brauer A, Muscheler R, Hansen F, Petrick C, Aldahan A,
37 Possnert G, van Geel B. (2012) Regional atmospheric circulation shifts induced by a grand solar
38 minimum. *Nature Geosci* 5:397-401. doi:10.1038/ngeo1460

- 1 Nielsen LC, De Yoreo JJ, DePaolo DJ (2013) General model for calcite growth kinetics in the
2 presence of impurity ions. *Geochim Cosmochim Acta* 115:100-114.
3 doi:10.1016/j.gca.2013.04.001
- 4 Scholz D, Hoffmann DL (2011) StalAge – An algorithm designed for construction of
5 speleothem age models. *Q Geochron.* 6:369-382 doi:10.1016/j.quageo.2011.02.002
- 6 Shen G, Wang W, Wang Q, Zhao J, Collerson K, Zhou C, Tobias PV (2002) U-Series dating of
7 Liujiang hominid site in Guangxi, Southern China. *J Hum Evol* 43:817-829.
8 doi:10.1006/jhev.2002.0601
- 9 Sinclair DJ, Banner JL, Taylor FW, Partin J, Jenson J, Mylroie J, Goddard E, Quinn T, Jocsón J,
10 Miklavič B (2012) Magnesium and strontium systematics in tropical speleothems from the
11 Western Pacific. *Chem Geol* 294–295:1-17. doi:10.1016/j.chemgeo.2011.10.008
- 12 Steinhilber F, Beer J, Fröhlich C (2009) Total solar irradiance during the Holocene.
13 *Geophysical Res Lett* 36:L19704. doi:10.1029/2009gl040142
- 14 Swindles GT, Plunkett G, Roe HM (2007) A delayed climatic response to solar forcing at 2800
15 cal. BP: multiproxy evidence from three Irish peatlands. *The Holocene* 17:177-182.
16 doi:10.1177/0959683607075830
- 17 Tooth AF, Fairchild IJ (2003) Soil and karst aquifer hydrological controls on the geochemical
18 evolution of speleothem-forming drip waters, Crag Cave, southwest Ireland. *J Hydrol* 273:51-
19 68. doi:10.1016/S0022-1694(02)00349-9
- 20 Treble P, Shelley JMG, Chappell J (2003) Comparison of high resolution sub-annual records of
21 trace elements in a modern (1911–1992) speleothem with instrumental climate data from
22 southwest Australia. *Earth Planet Sci Lett* 216:141-153. doi:10.1016/S0012-821X(03)00504-1
- 23 Tremaine DM, Froelich PN (2013) Speleothem trace element signatures: A hydrologic
24 geochemical study of modern cave dripwaters and farmed calcite. *Geochim Cosmochim Acta*
25 121:522-545. doi:10.1016/j.gca.2013.07.026
- 26 Triantaphyllou MV, Gogou A, Bouloubassi I, Dimiza M, Kouli K, Rousakis G, Kotthoff U,
27 Emeis KC, Papanikolaou M, Athanasiou M, Parinos C, Ioakim C, Lykousis V (2014) Evidence
28 for a warm and humid Mid-Holocene episode in the Aegean and northern Levantine Seas
29 (Greece, NE Mediterranean). *Reg Environ Change* 14:1697-1712. doi:10.1007/s10113-013-
30 0495-6
- 31 Trouet V, Esper J, Graham NE, Baker A, Scourse JD, Frank DC (2009) Persistent Positive
32 North Atlantic oscillation mode dominated the Medieval Climate Anomaly. *Science* 324: 78-80.
33 doi: 10.1126/science.1166349
- 34 Turrero MJ, Garralón A, Martín-Chivelet J, Gómez P, Sánchez L, Quejido A, Ortega AI,
35 Martín-Merino MA (2004) Seasonal changes in the chemistry of drip waters in Kaite Cave (N
36 Spain). In: Wanty RB, Seal II RS (Eds) *Water–Rock Interaction 11* Balkema Publishers London
37 pp 1407–1410
- 38 Turrero MJ, Garralón A, Gómez P, Sánchez L, Martín-Chivelet J, Ortega AI (2007)
39 Geochemical evolution of drip-water and present-growing calcite at Kaite Cave (N Spain). In:

- 1 Bullen TD, Wang YX (Eds) Water-Rock Interaction 12 Balkema Publishers Rotterdam pp
2 1187–1190
- 3 Turrero MJ, Garralón A, Sánchez L, Ortega AI, Martín-Chivelet J, Gómez P, Escribano A
4 (2015) Variations in Trace Elements of Drip Waters in Kaite Cave (N Spain): Significance in
5 Terms of Present and Past Processes in the Karst System. In: Andreo B, Carrasco F, Durán JJ,
6 Jiménez P, LaMoreaux JW (eds) Hydrogeological and Environmental Investigations in Karst
7 Systems, vol 1. Environ Earth Sci. Springer Berlin Heidelberg, pp 579-586. Springer-Verlag
8 Berlin Heidelberg 2015. doi 10.1007/978-3-642-17435-3_65
- 9 Vadillo JM, Vadillo I, Carrasco F, Laserna JJ (1998) Spatial distribution profiles of magnesium
10 and strontium in speleothems using laser-induced breakdown spectrometry. Fresenius J Anal
11 Chem 361:119-123. doi:10.1007/s002160050846
- 12 Vasiliev SS, Dergachev VA (2002) The ~2400-year cycle in atmospheric radiocarbon
13 concentration: bispectrum of ^{14}C data over the last 8000 years. Ann. Geophys 20 (1): 115–20.
14 doi:10.5194/angeo-20-115-2002
- 15 Wang Y, Cheng H, Edwards RL, He Y, Kong X1, An Z, Wu J, Kelly MJ, Dykoski CA, Li X
16 (2005) The Holocene Asian Monsoon: Links to Solar Changes and North Atlantic Climate.
17 Science 308:854-857. doi:10.1126/science.1106296
- 18 Wanner H, Mercolli L, Grosjean M, Ritz SP (2015) Holocene climate variability and change; a
19 data-based review. J Geol Soc 172:254-263 doi:10.1144/jgs2013-101
- 20 Wanner H, Solomina O, Grosjean M, Ritz SP, Jetel M (2011) Structure and origin of Holocene
21 cold events. Quaternary Sci Rev 30:3109-3123. doi:10.1016/j.quascirev.2011.07.010
- 22 Weiss H, Courty M-A, Wetterstrom W, Guichard F, Senior L, Meadow R, Curnow A (1993)
23 The Genesis and Collapse of Third Millennium North Mesopotamian Civilization. Science
24 261:995-1004. doi:10.1126/science.261.5124.995
- 25
- 26

1 **Figure Captions**

2 **Fig 1** a) Location map of the Kaite Cave in northern Spain. b) Longitudinal section of the
3 stalagmite Buda-100, used in this study, which was retrieved from the Buda Hall in the Kaite
4 Cave (Ojo Guareña Karst Complex, Burgos province).

5 **Fig 2** a) Experimental setup for the measurements by laser induced breakdown spectroscopy
6 (LIBS). (b) Example of polished thick section of the stalagmite used for LIBS measurements, in
7 which the microcraters produced by the laser beam on the sample can be observed. (c) Example
8 of spectrum obtained by LIBS, which results from the average of 20 laser pulses at each single
9 position. (d) Detail of the emission peaks, from which the Mg/Ca activity ratio is calculated.

10 **Fig 3** Experimental tests performed to check the quality and reliability of the analytical data
11 obtained by LIBS in the speleothem. (a) *Lateral homogeneity test*: The graph shows the Mg/Ca
12 intensity ratio measured in 12 points along a single growth layer of the stalagmite, performed to
13 check the lateral homogeneity. Note that the values are remarkably homogeneous except for the
14 points 3 and 4. As can be observed in the microphotograph, these two outliers are produced by a
15 small error in the positioning of the sample, which determined that the laser beam was focused
16 slightly out of the selected micrometric layer. These analyses average the Mg/Ca ratio of the
17 two successive layers. (b) *Replicability test*: Mg/Ca intensity ratios measured for 80 single
18 points along two transects parallel to the growth axis show excellent replicability of the
19 geochemical series. Minor differences between the two records are mainly due to the high
20 resolution of the LIBS micro-sampling and the high variability of the Mg/Ca ratios in the
21 stalagmite at that micrometric scale. (c) *Plasma temperature test*: The plasma temperature was
22 checked by monitoring the ratio of two atomic spectral lines in the LIBS experiment: Ca (I) at
23 430.8 nm and Ca (I) at 445.4 nm (ICa430.8/ICa445.4). The graphs show nearly constant
24 temperature of the plasma during the experimental measurements, which minimizes the matrix
25 effect and provides more accurate results. (d) Comparison of LIBS results with inductively
26 coupled plasma-optical emission spectroscopy (ICP-OES). The graph allows a visual
27 comparison of LIBS data performed for a segment of the stalagmite and the ICP-OES data
28 performed for the same interval. The correlation is very good, particularly if we consider the
29 strongly different amount of sample required for each analytical technique (milligrams in the
30 case of the ICP, few micrograms in the case of LIBS) and in the different lapse of time
31 represented in the analyzed sample in each case (10-20 years for the ICP vs. one year or less for
32 LIBS).

33 **Fig 4** A long-term (10 years) record of mean annual calcium concentration and Mg/Ca molar
34 ratio from dripwaters collected seasonally from two points of different drip-rate in Las Velas
35 Hall, Kaite Cave (N Spain) for the period 2002-2012. Dotted lines indicates the drip-rate
36 decreasing and Mg/Ca ratio increasing trends which are consistent with a long-term prior calcite
37 precipitation process as a consequence of a continuous decreasing of recharge in the area in the
38 time interval analyzed, as explained in the text.

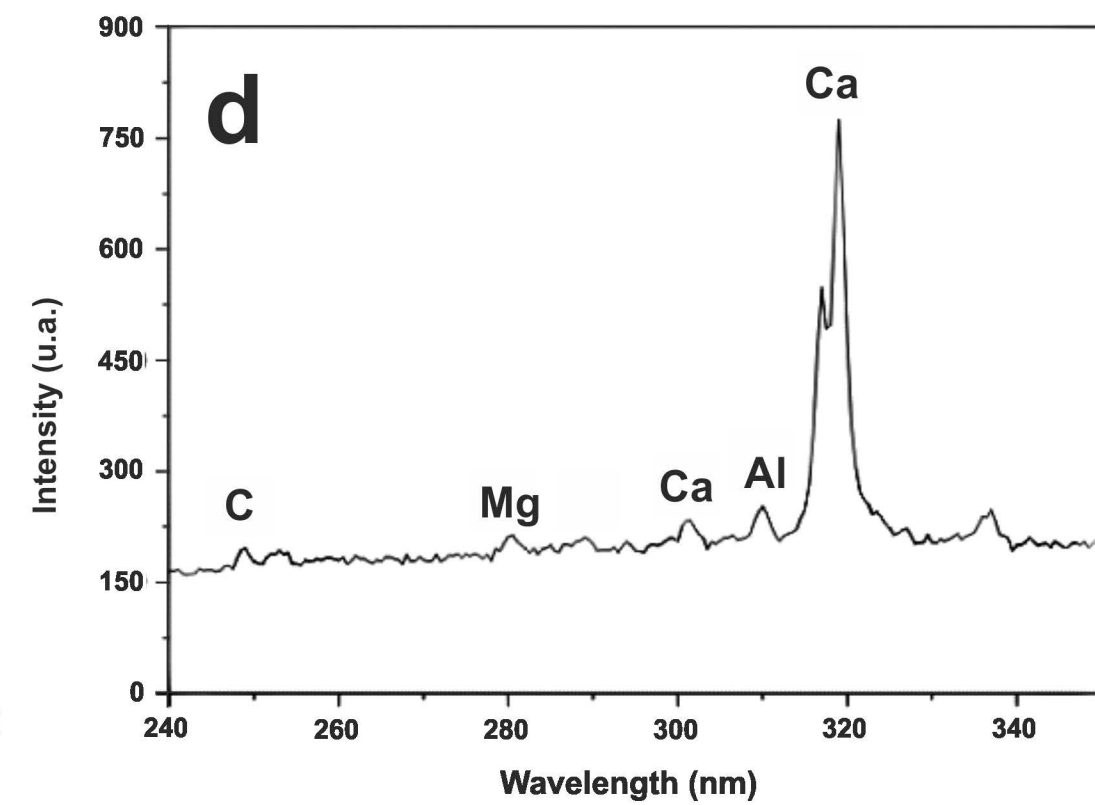
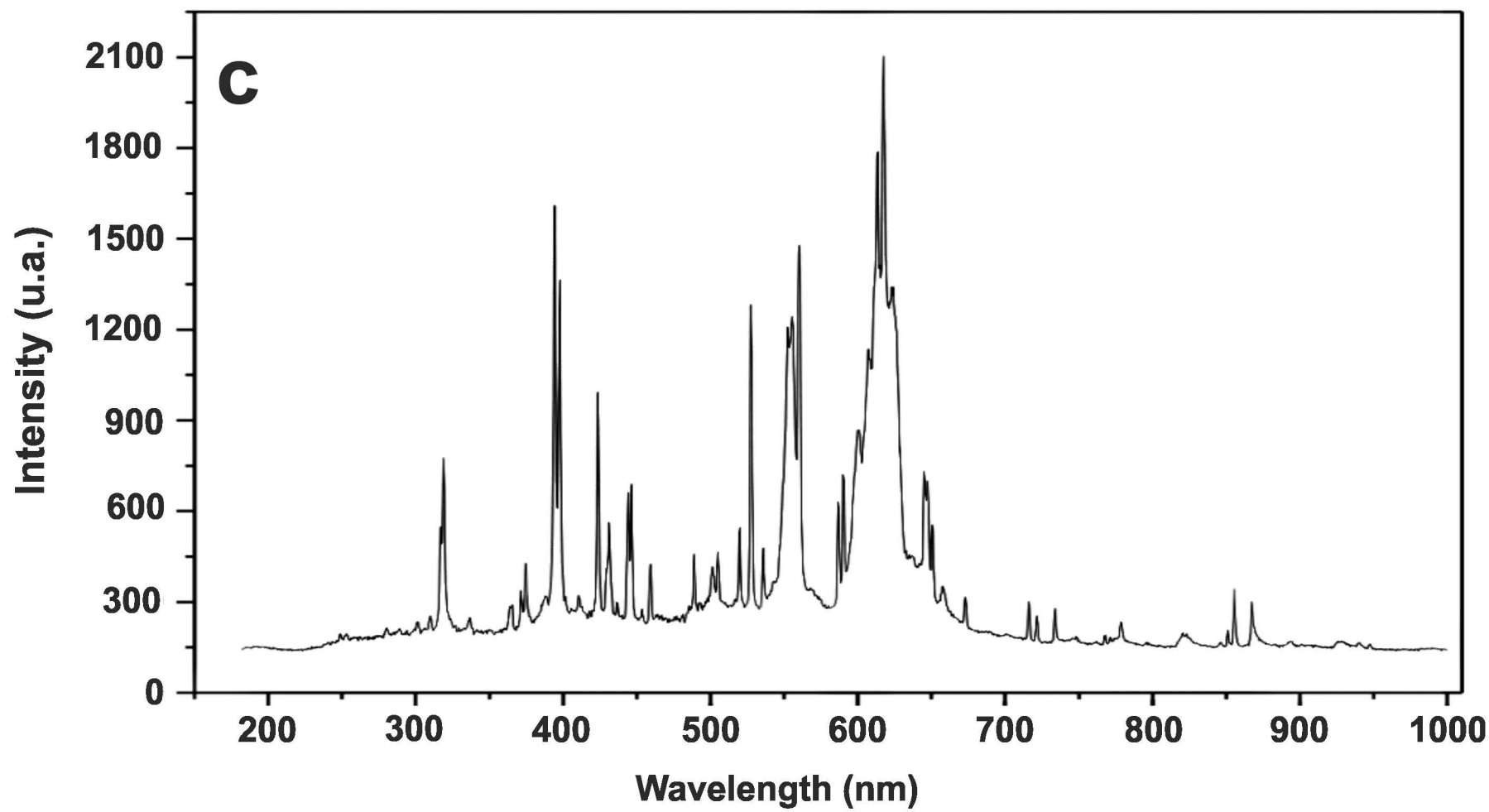
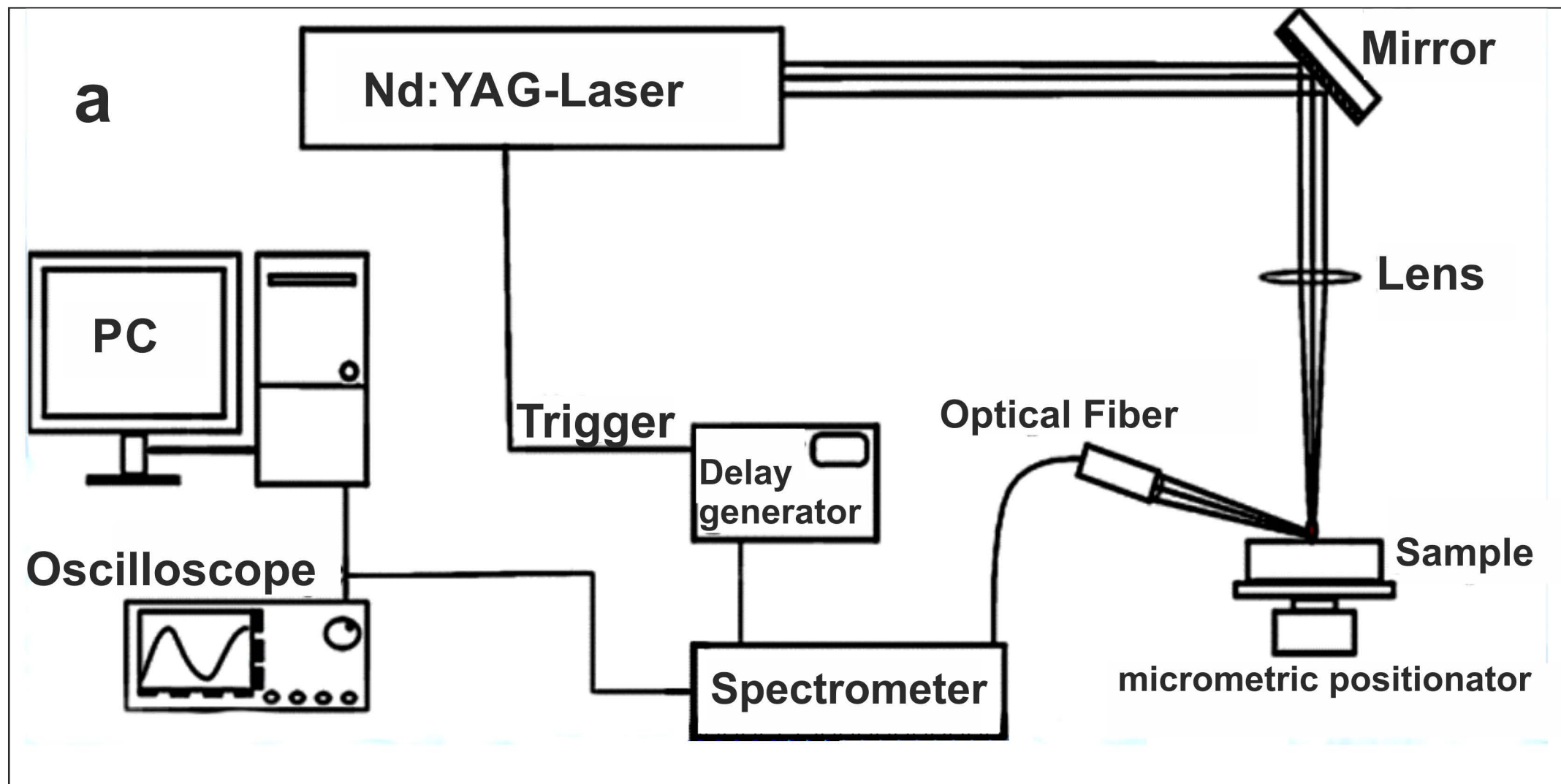
39 **Fig 5** Age depth model obtained with StalAge (Scholz and Hoffmann, 2011) for Buda-100
40 stalagmite, based on the ²³⁰Th ages of Table I.

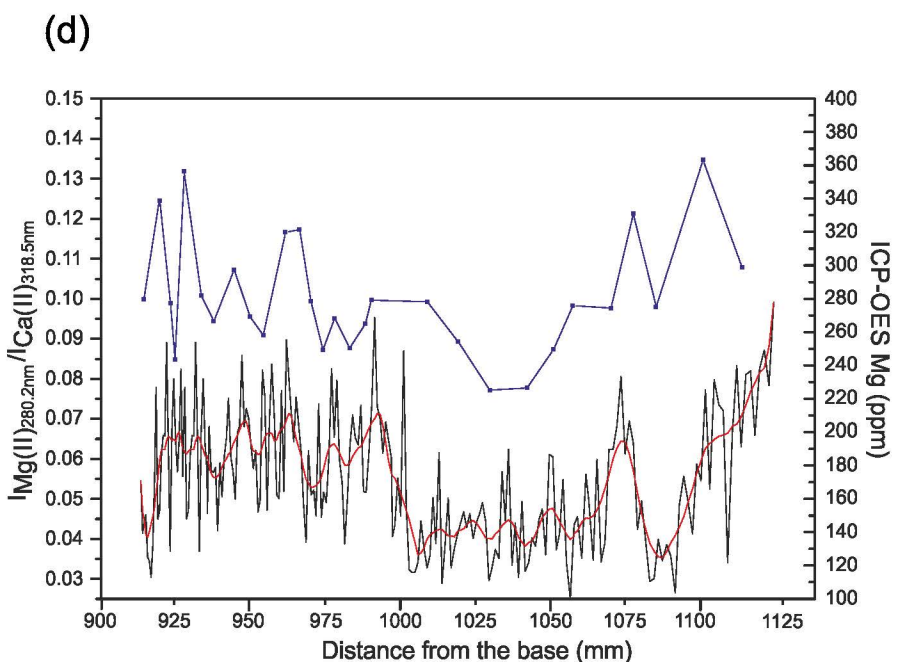
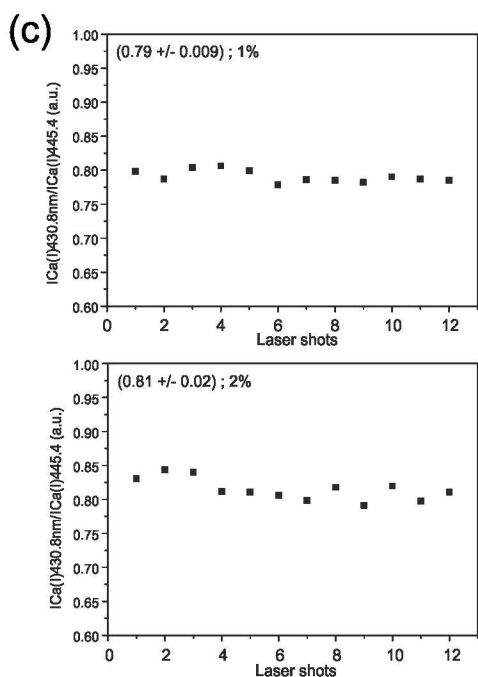
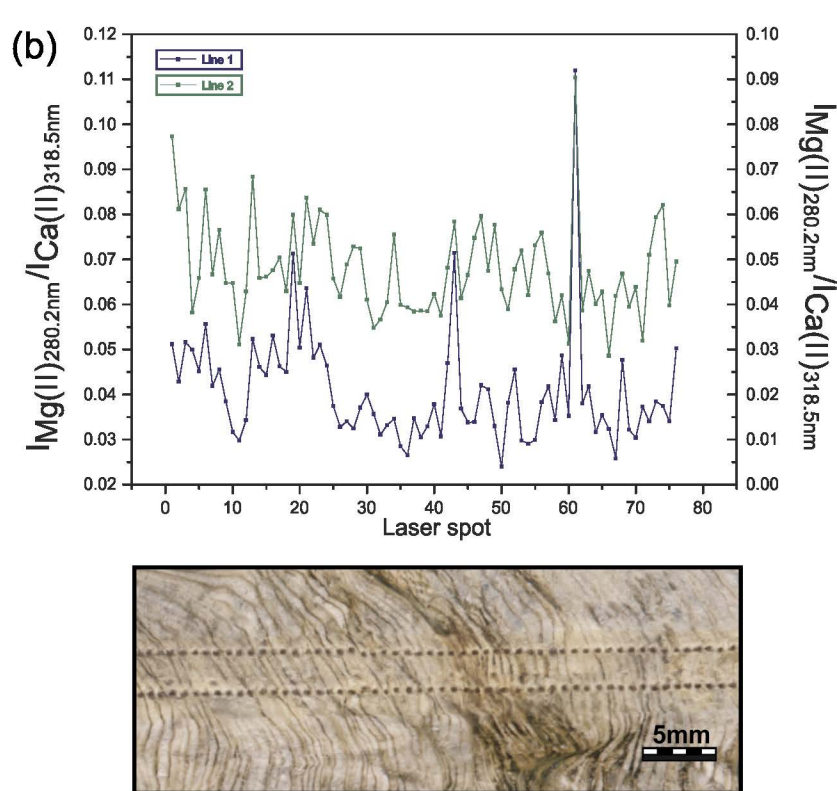
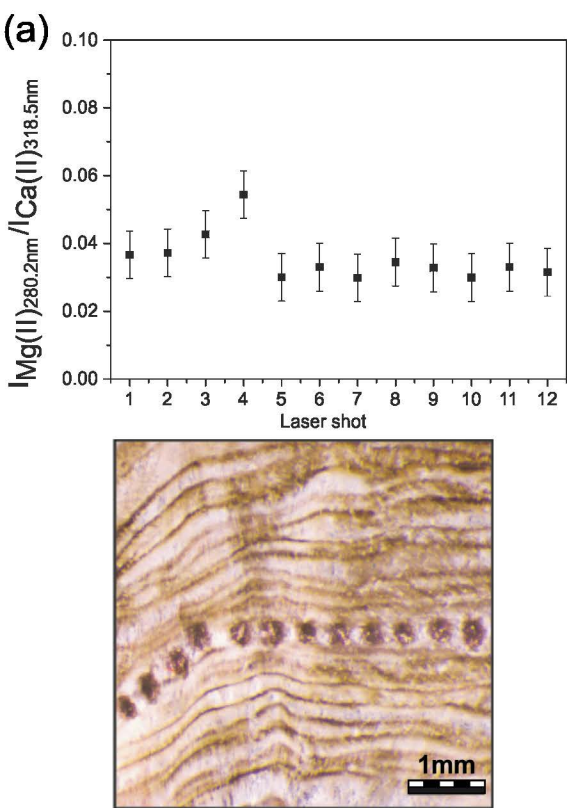
41 **Fig 6** Mg/Ca time series for stalagmite Buda-100, based in 2400 Mg/Ca measurements which
42 were time-scaled with the age model of Figure 5. The red line represents the 9-term running
43 average. The five main paleohydrological intervals described in the text and their general trends
44 are also shown. The Mg/Ca series is interpreted in terms of regional paleohydrological changes
45 through time (see text for discussion).

46 **Fig 7** Spectral diagram performed for the Mg/Ca series of stalagmite Buda-100. Spectral
47 analyses were performed with the Lomb periodogram algorithm, indicated for unevenly spaced
48 time series (PAST software, Hammer et al., 2006). Numbers labelled in the diagram indicate
49 periodicities (in ky) of the main spectral peaks. The 0.01 and 0.05 significance levels ("white
50 noise lines") are shown.

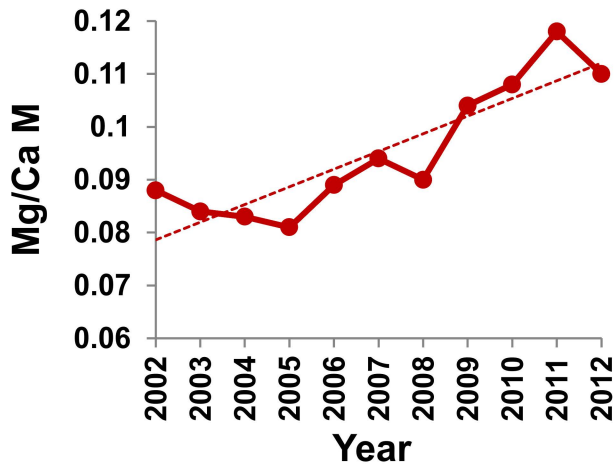


Figure 1 Cruz et al

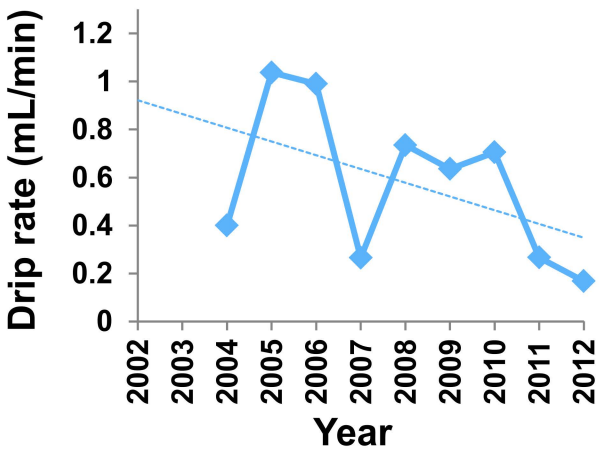
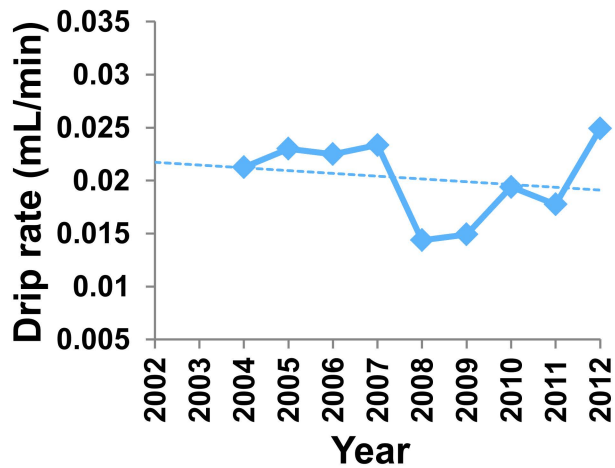
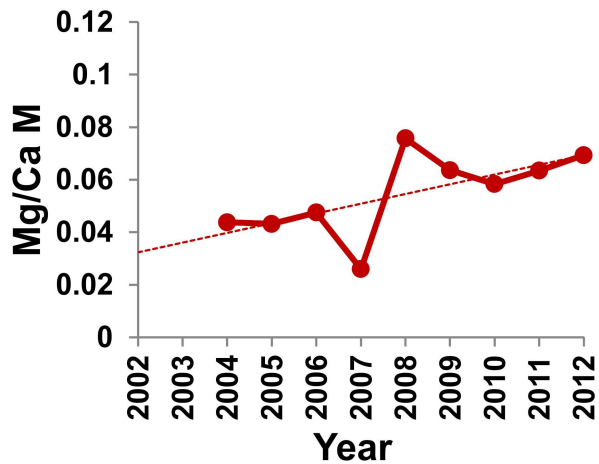


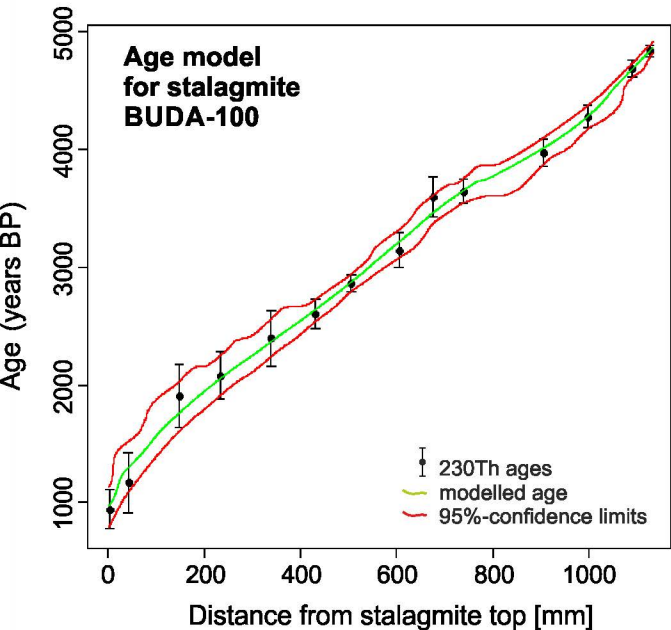


“slow” drip rate

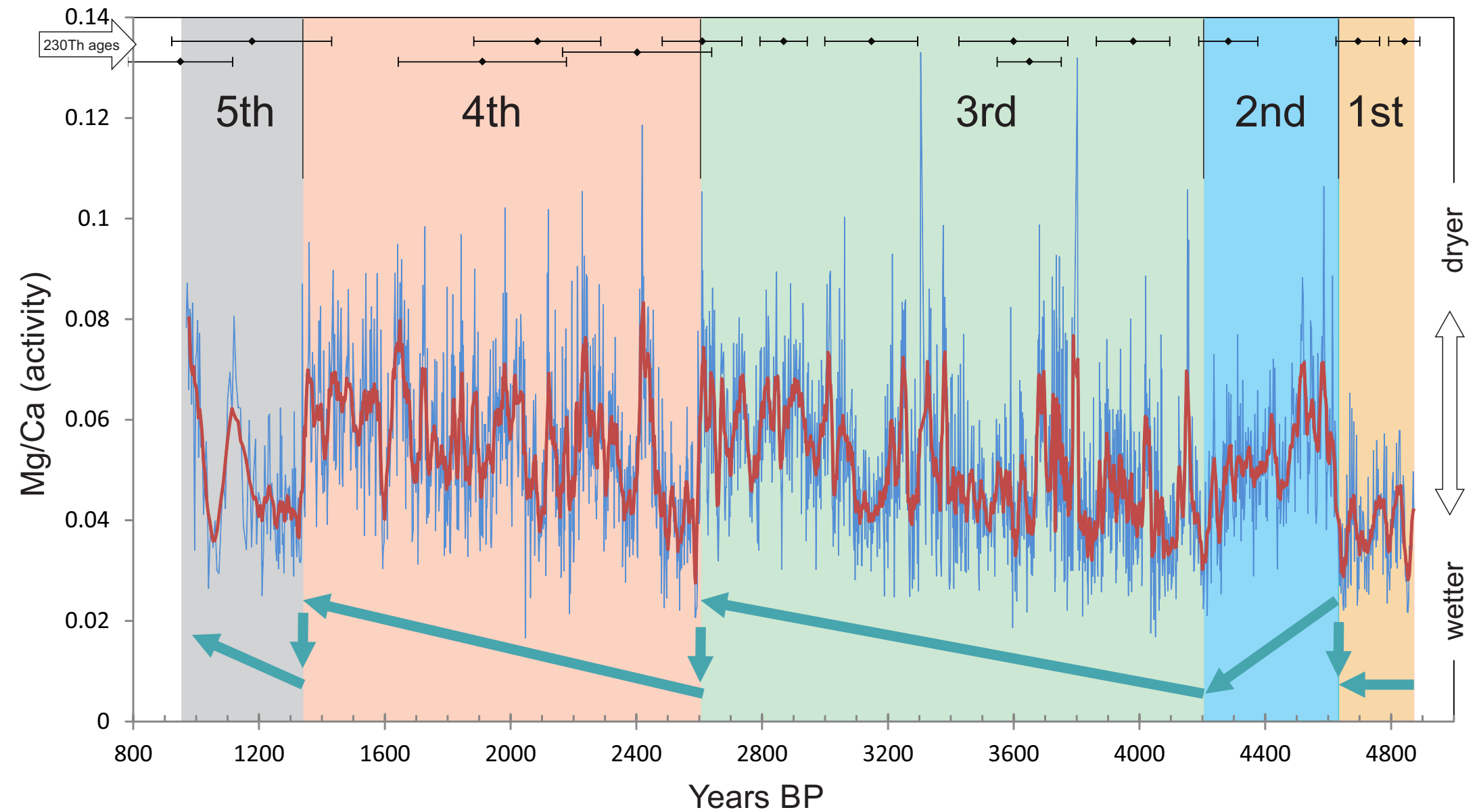


“rapid” drip rate





CRUZ ET AL FIGURE 5



CRUZ ET AL FIGURE 6

Mg/Ca Time series Stalagmite Buda-100

